



Synthesis, docking, and molecular dynamic study of hydrazones compounds to search potential inhibitor for breast cancer MCF-7

Jasril¹, Yuana Nurulita¹, Nur Afriana¹, Ihsan Ikhtiarudin², Neni Frimayanti²

¹Department of Chemistry, Faculty of Mathematic and Natural Sciences, Universitas Riau, Pekanbaru, 28293, Indonesia, ²Department of Pharmacy, Sekolah Tinggi Ilmu Farmasi (STIFAR), Jalan Kamboja, Pekanbaru, 28293 Indonesia

Corresponding Author:

Neni Frimayanti, Department of Pharmacy, Sekolah Tinggi Ilmu Farmasi (STIFAR), Jalan Kamboja, Pekanbaru, 28293 Indonesia. E-mail: nenifrimayanti@gmail.com

Received: Feb 05, 2021

Accepted: Mar 23, 2021

Published: Dec 04, 2021

ABSTRACT

Introduction: Hydrazones have been reported for various biological activities, such as anticancer. The presence of the azomethine group (-NHN=CH-) makes these compounds as one of the important classes in many synthetic products. **Objective:** The aim of this work is to explore the potential of halogenated hydrazones series as breast cancer inhibitors. **Methods:** In this study, some series of halogenated hydrazones have been synthesized through condensation reaction between halogenated benzaldehydes and phenylhydrazine under microwave irradiation. The structures of the halogenated hydrazones were confirmed by ultraviolet, fourier-transform infrared, NMR, and gas chromatography-mass spectrometry spectroscopic data. The *in silico* studies i.e. docking and molecular dynamic simulations were performed on these compounds (**3a-3i**) using CHARMM27 force field. Then, drug-likeness properties were calculated using Swiss-ADME server and the *in silico* toxicity prediction was performed using vNN-ADMET server. **Results:** Based on the combination of molecular docking, molecular dynamic, drug-likeness properties, and *in silico* toxicity studies, the compounds **3d** with chloro substituent in *ortho* position and compound **3i** with bromo substituent in *para* position showed good potency as active inhibitors for MCF-7 with lowest toxicity risk. **Conclusion:** This strategy is an early stage for discover new drugs for then it can be used as breast cancer inhibitors.

Keywords: Hydrazone, docking, molecular dynamic, MCF-7, breast cancer, druglikeness, toxicity prediction

INTRODUCTION

The development of new compound structures that have potential and have biological activities such as anti-inflammatory, anticancer, antimicrobial, antihypertensive, and other biological activities still remain to be the main objective by many researchers. Hydrazones possessing an azomethine -NHN=CH- group constitute an important class of compounds for new drug development. These compounds have been demonstrated to possess various biological activities. The search for antitumoral drugs led to the discovery of several hydrazones having antitumoral activity. Some phenolic and aryl hydrazones have been reported for their cytotoxicity in the range of 50–70% against MCF-7 and ZR-75-1 human malignant breast cell lines.^[1] Some hydrazinopyrimidine derivatives have also been demonstrated

inhibitory effect on the growth of a wide range of cancer cell lines^[2] and N-acylhydrazone compounds showed good antitumor activity.^[3] Other studies have also reported that some hydrazone derivative compounds have shown promising anticancer properties against A549 (lung cancer) and NIH3T3 (mouse embryonic fibroblast) cell line.^[4] In addition, the combinations of hydrazones with other functional groups form the other compounds with interesting physical and chemical properties. Therefore, the hydrazones are also widely used in organic synthesis as intermediate^[5] and also as target structure in drug discovery and drug design works.

The halogen substituents play some important roles in many anticancer researches. Most of halogenated aromatic compounds, such as halogenated flavonols,^[6] chalcones, and pyrazolines^[7,8] exhibited potential anticancer activity. In

addition, significant number of drugs and their candidates are halogenated compounds and we can find that some anticancer drugs also contain halogen atom.^[9] Therefore, in this work, we are interested to study the potency of halogenated hydrazones series as anticancer agent.

Computational chemistry plays an important role in the drug design work as well as in the mechanistic study by placing a molecule into the binding site of the target macromolecule in a noncovalent fashion.^[10] Docking and MD simulation technique will undoubtedly continue to play an important role in drug discovery.^[11] In this study, we synthesized some series of hydrazones contained halogens (fluoro, chloro, and bromo) substituent under microwave irradiation. Then, the *in silico* studies were applied for predicting the inhibitory activity for breast cancer.

MATERIALS AND METHODS

General Informations

The materials used in this work were florobenzaldehyde, chlorobenzaldehyde, bromobenzaldehyde, methoxybenzaldehyde, phenylhydrazine, sodium hydroxide, hydrochloric acid, ethanol, methanol, 1,1-diphenyl-2-picrylhydrazyl, and ascorbic acid. All materials were obtained either from Merck (Merck KGaA, Darmstadt, Germany) or Sigma-Aldrich (Sigma-Aldrich Corp., St. Louis, MO, USA), and used without further purification.

Melting points were determined using Fisher Johns melting point apparatus (SMP 11-Stuart®). ultraviolet (UV) spectra were recorded on UV-visible spectrophotometer (Genesys 10S UV-visible v4.002 2L9N175013). IR spectra were recorded on fourier-transform infrared (FTIR) spectrophotometer (FTIR Shimadzu, IR Prestige-21). ¹H NMR spectra were recorded on NMR spectrometer (Agilent 500 MHz by DD2 console system). Mass spectra were measured on Gas chromatography-mass spectrometry (GC-MS) spectrometer (Agilent 6890 GC). Chemical purities of the compounds were checked by TLC analysis performed on silica gel GF254 (Merck) and by HPLC analysis (UFLC Prominence-Shimadzu LC solution, Detector UV SPD 20AD). The *in silico* study was performed by MOE software package (Chemical Computing Group).

General Procedures

General procedure for the synthesis of halogenated hydrazone series 3a-3i

The synthesis of halogenated hydrazone series (**3a-3e**, **3g**, and **3i**) in this work was performed by modification of previous literatures^[12-14] and the synthesis of compounds **3f** and **3h** have been reported in our previous work.^[15,16] The synthesis route of the halogenated hydrazone series is depicted in Figure 1 and the comparisons between this work and previous works were presented in Table 1. Some phenylhydrazine (3 mmol) was dissolved in 2 mL of absolute ethanol and then it was added by 2 mL of NaOH 3N and was homogenized. Then, each substituted benzaldehyde (1 mmol) was added and the mixture was irradiated (300 W) for 1–4 min. The progress of reaction was observed every minute by TLC analysis. If the reaction was finished, the mixture was neutralized by HCl 3N and cooled in an ice bath in a

refrigerator for 24 h to maximize the formation of precipitate. Then, the precipitate was separated by vacuum filtration and washed by cold distilled water and n-hexane to afford a pure product. Some crude products were recrystallized from ethanol to afford the pure product and compound **3b-3e** were resynthesized using 2 mL of glacial acetic acid (AcOH) as catalyst to afford the better yield.

1-(2-Fluorobenzylidene)-2-phenylhydrazine (3a)

The product was obtained as pink solid. Yield: 68,00%, m.p. 80°C, UV (EtOH): λ_{\max} = 209, 228, 300 and 354 nm. FTIR (KBr, cm^{-1}): 3308 (N-H str.), 3054 (Ar C-H str.), 1602 (C=N str.), 1516 and 1446 (Ar C=C str.), 1262 (C-N str.), 754 (C-F str.). ¹H-NMR (500 MHz, CDCl_3) δ (ppm): 8.03 (t, 1H, J = 8 Hz, Ar-H); 7.94 (s, 1H, azomethine H); 7.79 (br-s, 1H, NH); 7.29 (m, 3H, Ar-H); 7.18 (t, 1H, J = 7.5 Hz, Ar-H); 7.14 (d, 2H, J = 7.5 Hz, Ar-H); 7.06 (dd, 1H, J_1 = 11 Hz, J_2 = 9 Hz, Ar-H); 6.91 (t, 1H, J = 7.5 Hz, 1H, Ar-H). GC-MS: t_R = 11.176 min, the calculated exact mass of $\text{C}_{13}\text{H}_{11}\text{FN}_2$ = 214.1, $[\text{M}]^+$ was found at m/z = 214.1 (100%).

1-(3-Fluorobenzylidene)-2-phenylhydrazine (3b)

The product was obtained as pink crystal. Yield: 29.70%, m.p. 108–109°C, UV (EtOH): λ_{\max} = 206, 237, 301 and 350 nm. FTIR (KBr, cm^{-1}): 3311 (N-H str.), 3054 (Ar C-H str.), 1595 (C=N str.), 1516 and 1446 (Ar C=C str.), 1275 (C-N str.), 752 (C-F str.). ¹H-NMR (500 MHz, CDCl_3) δ (ppm): 7.69 (br-s, 1H, NH); 7.64 (s, 1H, azomethine H); 7.43 (d, 1H, J = 10 Hz, Ar-H); 7.33 (m, 4H, Ar-H); 7.13 (d, 2H, J = 7.5 Hz, Ar-H); 7.00 (t, 1H, J = 8 Hz, Ar-H); 6.92 (t, 1H, J = 7 Hz, Ar-H). GC-MS: t_R = 11.176 min, the calculated exact mass of $\text{C}_{13}\text{H}_{11}\text{FN}_2$ = 214.1, $[\text{M}]^+$ was found at m/z = 214.1 (100%).

1-(4-Fluorobenzylidene)-2-phenylhydrazine (3c)

The product was obtained as brown solid. Yield: 3.1% (NaOH as catalyst) and 77.67% (AcOH as catalyst), m.p. 120–121°C, UV (EtOH): λ_{\max} = 207, 227, 299, 343 nm. FTIR (KBr, cm^{-1}): 3311 (N-H str.), 3053 (Ar C-H str.), 1603 (C=N str.), 1506 and 1446 (Ar C=C str.), 1245 (C-N str.), 755 (C-F str.). ¹H-NMR (500 MHz, CDCl_3) δ (ppm): 7.68 (s, 1H, azomethine H); 7.65 (dd, 2H, J_1 = 8.5 Hz, J_2 = 5.5 Hz, Ar-H-2', Ar-H-6''); 7.62 (br-s, 1H, NH); 7.29 (t, 2H, J = 8 Hz, Ar-H-3'', Ar-H-3'', Ar-H-5''); 7.12 (d, 2H, J = 8 Hz, Ar-H-2'', Ar-H-6''); 7.08 (t, 2H, J = 8.5 Hz, Ar-H-3', Ar-H-5'); 6.89 (td, 1H, J_1 = 7 Hz, J_2 = 1 Hz, Ar-H-4''). ¹³C-NMR (125 MHz, CDCl_3) δ (ppm): 162.62 (d, $^1J_{\text{C-F}}$ = 161.25 Hz, C-4''); 144.58 (C-1''); 136.04 (C-1); 131.52 (C-1'); 129.30 (2C, C-3'', C-5''); 127.74 (d, 2C, $^3J_{\text{C-F}}$ = 7.5 Hz, C-2', C-6'); 120.18 (C-4''); 115.65 (d, 2C, $^2J_{\text{C-F}}$ = 22.5 Hz, C-3', C-5'); 112.72 (2C, C-2'', C-6''). GC-MS: t_R = 9.225 min, the calculated exact mass of $\text{C}_{13}\text{H}_{11}\text{FN}_2$ = 214.1, $[\text{M}]^+$ was found at m/z = 214.1 (100%).

1-(2-Chlorobenzylidene)-2-phenylhydrazine (3d)

The product was obtained as brown crystal. Yield: 19.56% (NaOH as catalyst) and 96.23% (AcOH as catalyst), m.p. 70°C, UV (EtOH): λ_{\max} = 209, 249, 302 and 355 nm. FTIR (KBr, cm^{-1}):

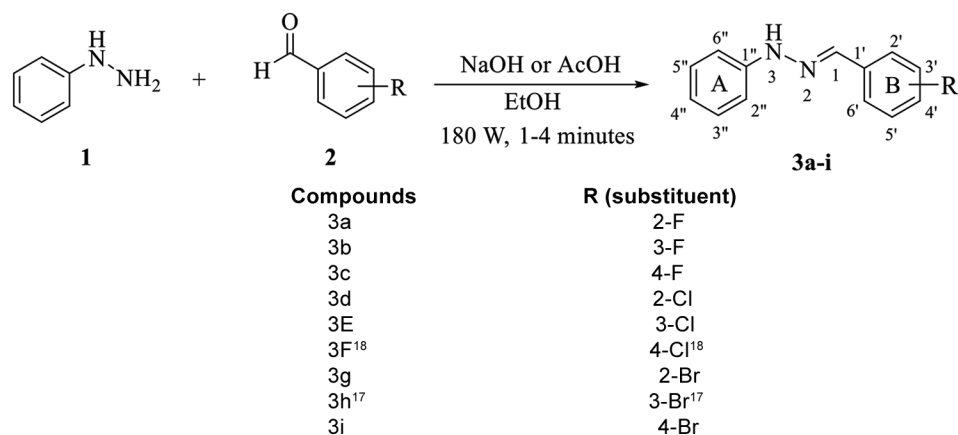


Figure 1: Synthesis route of the halogenated hydrazone series 3a-i. a) Afriana et al.,^[17] b) Jasril et al.^[18]

Table 1: The comparison between this work and the other previous work

Literatures	Substituents	Synthesis methods	Catalyst	Reaction times	Allowed in RT	Yield
[9]	4-OCH ₃	Refluxed in MeOH	-	45 min	72 h	Not reported
[10]	2-NO ₂	Refluxed in MeOH	-	25 min	48 h	Not reported
[11]	4-Cl	Refluxed in MeOH	-	30 min	72 h	Not reported
Previously work [e]		Irradiated in EtOH	AcOH	2 min	24 h ^{a)}	85%
Previously work [f]	3-Br	Irradiated in EtOH	KOH	2 min	24 h ^{a)}	90.18%
This work	2-F, 3-F, 4-F, 2-Cl, 3-Cl, 4-Cl, 2-Br, 4-Br	Irradiated in EtOH	NaOH	5 min	24 h ^{a)}	3.10–68.00%
	4-F, 2-Cl	Irradiated in EtOH	AcOH	5 min	24 h ^{a)}	77.67–96.23%

a) The reaction mixture was allowed in ice bath in a refrigerator

3316 (N-H str.), 3053 (Ar C-H str.), 1604 (C=N str.), 1519 and 1445 (Ar C=C str.), 1250 (C-N str.), 754 (C-Cl str.). ¹H-NMR (500 MHz, CDCl₃) δ (ppm): 8.12 (s, 1H, azomethine H); 8.09 (dd, 1H, Ar-H); 7.86 (br-s, 1H, NH); 7.36 (d, 1H, *J* = 8 Hz, Ar-H); 7.29 (m, 3H, Ar-H); 7.23 (td, 1H, Ar-H); 7.14 (d, 2H, *J* = 9.5 Hz, Ar-H); 6.91 (t, 1H, *J* = 7 Hz, Ar-H). GC-MS: *t*_R = 12.330 min, the calculated exact mass of C₁₃H₁₁ClN₂ = 230.1, [M]⁺ and [M+2]⁺ were found at *m/z* = 230.1 (100%) and 232.1 (32%), respectively.

1-(3-chlorobenzylidene)-2-phenylhydrazine (3e)

The product was obtained as pink crystal. Yield: 69.54%, m.p. 120°C, UV (EtOH): λ_{max} = 208, 249, 301, and 354 nm. FTIR (KBr, cm⁻¹): 3323 (N-H str.), 3053 (Ar C-H str.), 1585 (C=N str.), 1516 and 1441 (Ar C=C str.), 1250 (C-N str.), 748 (C-Cl str.). ¹H-NMR (500 MHz, CDCl₃) δ (ppm): 7.68 (br-s, 1H, NH); 7.61 (s, 1H, azomethine H); 7.49 (d, 1H, *J* = 7.5 Hz, Ar-H); 7.29 (m, 5H, Ar-H); 7.13 (d, 2H, *J* = 7.5 Hz, Ar-H); 6.91 (t, 1H, *J* = 7 Hz, Ar-H). GC-MS: *t*_R = 12.492 min, the calculated exact mass of C₁₃H₁₁ClN₂ = 230.1, [M]⁺ and [M+2]⁺ were found at *m/z* = 230.1 (100%) and 232.1 (31.02%), respectively.

1-(2-Bromobenzylidene)-2-phenylhydrazine (3g)

The product was obtained as orange crystal. Yield: 23.10%, m.p. 64°C, UV (EtOH): λ_{max} = 209, 249, 301, and 354 nm.

FTIR (KBr, cm⁻¹): 3298 (N-H str.), 3053 (Ar C-H str.), 1604 (C=N str.), 1516 and 1480 (Ar C=C str.), 1270 (C-N str.), 751 (C-Br str.). ¹H-NMR (500 MHz, CDCl₃) δ (ppm): 8.09 (d, 1H, *J* = 7.5 Hz, Ar-H); 8.07 (s, 1H, azomethine H); 7.87 (br-s, 1H, NH); 7.55 (d, 1H, *J* = 9 Hz, Ar-H); 7.32 (m, 3H, Ar-H); 7.15 (m, 3H, Ar-H); 6.92 (t, 1H, *J* = 7 Hz, Ar-H). GC-MS: *t*_R = 12.971 minutes, the calculated exact mass of C₁₃H₁₁BrN₂ = 274.0, [M]⁺ and [M+2]⁺ were found at *m/z* = 274.1 and 276.1 (64.16%), respectively.

1-(4-Bromobenzylidene)-2-phenylhydrazine (3i)

The product was obtained as pink crystal. Yield: 42.16%, m.p. 104°C, UV (EtOH): λ_{max} = 210, 243, 344, and 354 nm. FTIR (KBr, cm⁻¹): 3305 (N-H str.), 3052 (Ar C-H str.), 1593 (C=N str.), 1518 and 1485 (Ar C=C str.), 1265 (C-N str.), 757 (C-Br str.). ¹H-NMR (500 MHz, CDCl₃) δ (ppm): 7.67 (br-s, 1H, NH); 7.62 (s, 1H, azomethine H); 7.53 (d, 2H, *J* = 9 Hz, Ar-H-2, Ar-H-6); 7.50 (d, 2H, *J* = 9 Hz, Ar-H-3, Ar-H-5); 7.30 (t, 2H, *J* = 8 Hz, Ar-H-3, Ar-H-5); 7.12 (d, 2H, *J* = 7.5 Hz, Ar-H-2, Ar-H-6); 6.91 (t, 1H, *J* = 7.5 Hz, Ar-H-4). ¹³C-NMR (125 MHz, CDCl₃) δ (ppm): 144.36 (C-1); 135.80 (C-1); 134.31 (C-1); 131.76 (2C, C-3, C-5); 129.35 (2C, C-3, C-5); 127.54 (2C, C-2, C-6); 122.18 (C-4); 120.40 (C-4); 112.81 (2C, C-2, C-6). GC-MS: *t*_R = 11.388 min, the calculated exact mass of C₁₃H₁₁BrN₂ = 274.0, [M]⁺ and [M+2]⁺ were found at *m/z* = 274.1 and 276.1 (100%), respectively.

In silico Studies

Protein preparation

Protein tyrosine kinase was observed from protein databank (RSCB PDB) homepage with pdb ID 1t46. Preparation of protein was begun with removing original ligand from the oriental protein, following with added hydrogen atom. The next step is a minimization of alpha carbon atom, backbone atom minimized, and finally minimization for whole molecule protein. The minimization process was performed using the same force field i.e. CHARMM27 with distances of 0.01.

Ligand preparation

Nine ligand [Figure 2] and doxorubicin was sketched using chemDraw software for then all the ligands were copied into discovery studio visualizer following with copied the files into MOE. All the ligands were inserted into mdb database in MOE software packages (Chemical computing group) for then its can be used to perform docking simulation.

Molecular docking

Docking was performed using MOE (Chemical computing group, CCG) software packages. It was started with setting the potential set up by using CHARMM27 force field with gridbox among radius x, y, and z of 67, 86, 66, respectively. Refinement was set into 100. The best poses of docking results were selected based on some parameters such as binding free energy, root mean square deviation (RMSD), and also factor of binding (the same binding interaction with positive control).

Molecular dynamic simulation

Preliminary studies of molecular dynamic simulation was performed using NAMD (NANoscale Molecular Dynamics program v 2.9) software package. CHARMM27 (Chemistry at HARvard Macromolecular Mechanics) was selected as the best force field. TIP3P water box with 2.5 Å water layer for each direction of coordinated structure was used to achieve modeled protein.

The gradual system was heated using NVT ensemble from 0 to 300 K over 100 ps. Time scaling was settled on 50 ns time scale for each system in an isothermal isobaric ensemble (NPT) with periodic boundary conditions. Temperature and pressure parameters were set on 1.0 ps. The sampling process was saved the coordinates for every 0.1 ps. Binding free energy calculations and hydrogen bonding distance will be selected as a parameter to generated the best conformations of MD simulation.

Generation of pharmacophore

The pharmacophore query editor tool was applied to develop the pharmacophore properties for these synthesized compounds. It was used to determine the features of the pharmacophore and also to generate the hypothesis for the alignments of this pharmacophore. In this research, the alignments of this pharmacophore were achieved using three of the best features i.e. hydrophobic, hydrogen bond donor, and aromatic ring).

Drug-likeness properties calculation

The drug-likeness properties of halogenated hydrazone series was calculated using Swiss-ADME server (<http://www.swissadme.ch>) followed the previous literature.^[19]

In silico toxicity prediction

The *in silico* toxicity prediction was performed using vNN-ADMET server (<https://vnnadmet.bhsai.org>) followed by previous literature^[20] to predict hepatotoxicity, cardiotoxicity, mitochondrial toxicity, mutagenicity, and maximum recommended therapeutic dose (MRTD).

RESULTS AND DISCUSSION

Synthesis of Compound 3a-i

The synthesis of hydrazones series in this work has been performed through condensation reaction between

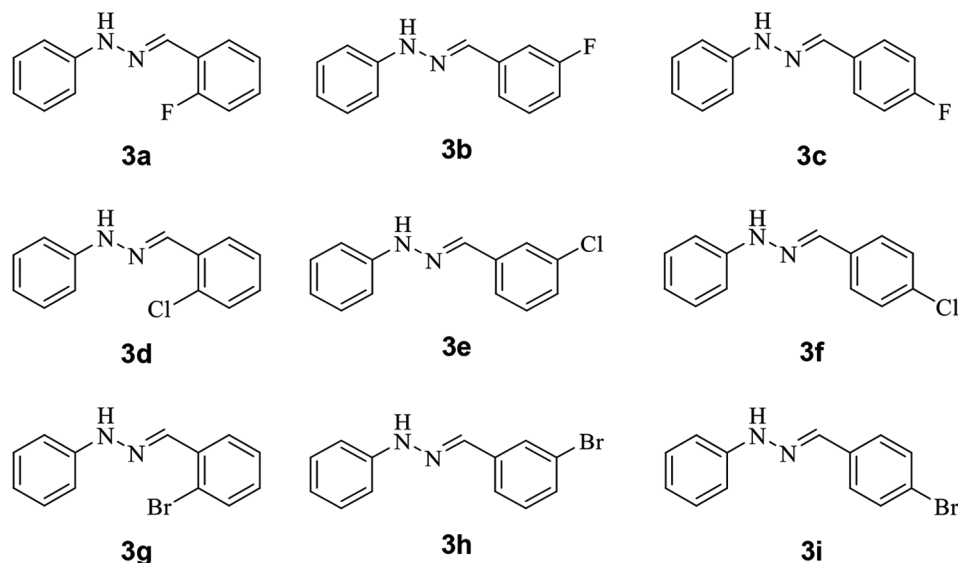


Figure 2: Molecular structure of substituted hydrazone 3a-3i used as ligands

phenylhydrazine (1) with substituted benzaldehydes (2) by modification of the previous method.^[12-14] In the previous method, the synthesis of hydrazone was performed by conventional heating, under reflux in methanol for 25–45 min, and then allowed in room temperature for 48–72 h. In this work, the synthesis was performed under microwave irradiation for 5 min with the presence of sodium hydroxide as a catalyst, and only need additional time of 24 h in ice bath to maximize the precipitate formation. This modified method has been proved to save time and ethanol as more preferable solvent and more environmentally friendly than methanol. However, this method seems very incompatible for compound **3c** (3.1%) and **3d** (19.56%). However, we have re-synthesized both compounds **3c** and **3d** using another method (microwave irradiation in ethanol and glacial acetic acid as a catalyst), and we afford 77.67 and 96.23% yield for **3c** and **3d**, respectively. Based on this result, we conclude that the use of acetic glacial acid is more suitable than sodium hydroxide for the synthesis of halogenated hydrazone series. All the spectroscopic data, including UV, FT-IR, NMR, and GCMS agreed with the structure of the products.

The formation of the azomethine group in hydrazone series has been confirmed by FTIR analysis. The FTIR spectra of synthesized compound showed the absorption band around 3300 cm⁻¹ that indicated the presence of N-H bond in the azomethine group. In addition, the absorption bands from C=N bond in azomethine group were appeared around 1600 cm⁻¹. The ¹H-NMR spectra of all halogenated hydrazone series also confirmed the formation of azomethine group by the appearance of broad singlet signal (N-H proton) around δ 7.50–7.60 ppm and singlet signal (methine proton) around δ 7.62–7.80 ppm. Overall, the ¹H-NMR spectra of the synthesized compounds showed the number of protons corresponded to be expected molecule targets.

The 2D NMR analysis was also performed for para halogenated hydrazone series. The HSQC analysis was performed to provide the information about ¹H-¹³C correlations between the protons directly bonded to the carbon atom in a molecule. In addition, the HMBC analysis was also performed to provide information about ¹H-¹³C correlations between a proton with several carbon atoms that are separated by two till three bonds. Based on both HSQC and HMBC analysis, all protons and carbons showed matching correlation to the expected structures (See supplementary

materials). Then, the mass of hydrazone series was also established by GC-MS analysis. The GC chromatogram showed that the synthesized compounds possess high purity and the MS spectra showed the molecular ion peak [M]⁺ at m/z 214.1 for fluoro substituted hydrazones, m/z 230.1 and 232.1 (3:1) for chloro substituted hydrazones, m/z 274.1 and 276.1 (1:1) for bromo substituted hydrazones. These molecular ion peaks expressed the molecular mass of the synthesized compound. Overall, the spectroscopic data agreed with the structure expected.

Molecular Docking

Docking results of these ligands are depicted in Table 2. According to the docking results, doxorubicin was used as positive control has the lowest binding free energy of -30.9 kcal/mol. In addition, doxorubicin has interaction via hydrogen bond through residue amino acid such as Tyr672 and Asp677. Van der Waals interaction was also constructed between this doxorubicin and residue amino acids Cys673, Gly676, Tyr675, Cys674, Asn689 and Phe811. Unfortunately, doxorubicin was not able to build any binding with hydrophobic amino acid. Figure 3 is depicted the spatial arrangement of doxorubicin.

Molecule **3a** and **3h** have binding free energy of -20.68 kcal/mol and -18.23 kcal/mol, respectively. In addition, these molecules were constructed hydrogen bond through amino acid Lys623. The existence of the hydrogen bonding in this complex was shown that molecules **3a** and **3h** have another spatial mode of arrangement. An important amino acid interaction was performed through van der Waals interaction, i.e., Glu640 and Asp810. Although these molecules have an RMSD less than two, there is a factor of binding (i.e. the same sequence of amino acid-like positive control). This is indicated that molecule **3a** and **3h** was unable to be inhibitor for the MC7 cell line. The spatial arrangement for those molecules is presented in Figure 4.

Molecule **3b** and **3c** have three types of interaction with amino acid. This molecule has hydrogen bond interaction via amino acid Lys623, van der Waals interaction through Glu640 and Asp810 and also hydrophobic interaction through Lys623 and His790. In addition, molecule **3b** and **3c** have binding free energy of -17.13 kcal/mol and -22.09 kcal/mol, respectively. The presence of amino acids with different sequences such as positive control coupled with the high value of bond-free

Table 2: Docking results

Compounds	Binding free energy (kcal/mol)	RMSD	Hydrogen bond	VDW	Hydrophobic
3a	-20.68	0.00	Lys623	Glu640, Asp810	Lys623
3b	-17.13	0.00	Lys623	Glu640, Asp810	Lys623, His790
3c	-22.09	0.00	Lys623	Glu640, ASP810	Lys623, His790
3d	-27.98	0.00	His790, Arg791	Asp810	His790, Arg791
3e	-20.01	0.00	Lys623	Glu640, Asp810	Lys623, Asp810
3f	-16.45	0.00	Lys623	Glu640, Asp810	Lys623, Asp810
3g	-28.76	0.00	His790, Arg791	Asp810	His790, Arg791
3h	-18.23	0.00	Lys623	Glu640, Asp810	Lys623
3i	-28.59	0.00	His790, Arg791	Glu640, Asp810	His790, Arg791

energy, it may be caused this compound are estimating to be inactive as an MCF-7 inhibitor. Figure 5 is presented the spatial arrangement of compound **3b** and **3c**.

The same case for molecules **3e** and **3f** which are estimated to be inactive compounds, this is not only because the sequence of amino acid is different like the positive control but also because of the high value of binding free energy of -20.01 kcal/mol and -16.45 kcal/mol, respectively. Different sequence with positive control causes these molecules to

create another spatial arrangement, in addition, high binding free energy indicated that binding between complex ligand and protein is unstable. This presumably that both of these compounds become inactive inhibitors for MCF-7. Figure 6 are presented the spatial arrangement of compounds **3e** and **3f**.

Molecule **3d**, **3f**, and **3h** have the lower binding free energy than doxorubicin. The interactions between ligands and proteins through hydrogen bonds with His790 and Asp810. Van der waals interaction is also exists with Asp810 and hydrophobic bonds with amino acid sequences are not so different like positive control or it is still in range of the positive control sequence. The binding free energy of these compounds was also close with doxorubicin as positive control [Figure 7A and B]. It is indicated the high stability of these molecules. In addition, RMSD value of these molecules was less than two. the lower RMSD value indicated the smaller the errors that are made during the docking process. Thus, it may be the reason molecules **3d**, **3f**, and **3h** are estimated to have a big chance become active inhibitor.

The binding orientation of the estimated active compounds **3d**, **3f**, and **3h** were checked using superimpose. Based on the superimpose results, it seemed that three of these compounds have the same orientation with the protein. In addition, the superimpose was used to validate the docking results between

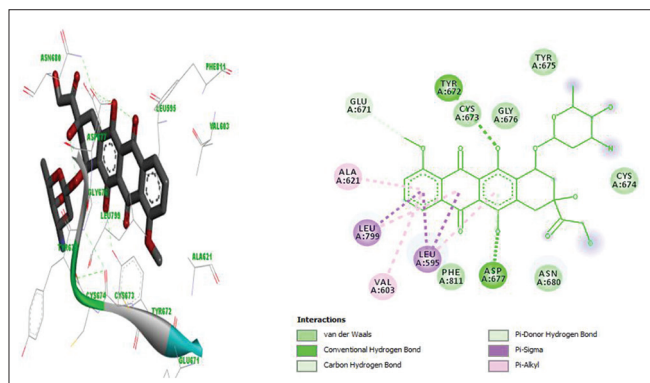


Figure 3: Spatial arrangement of doxorubicin

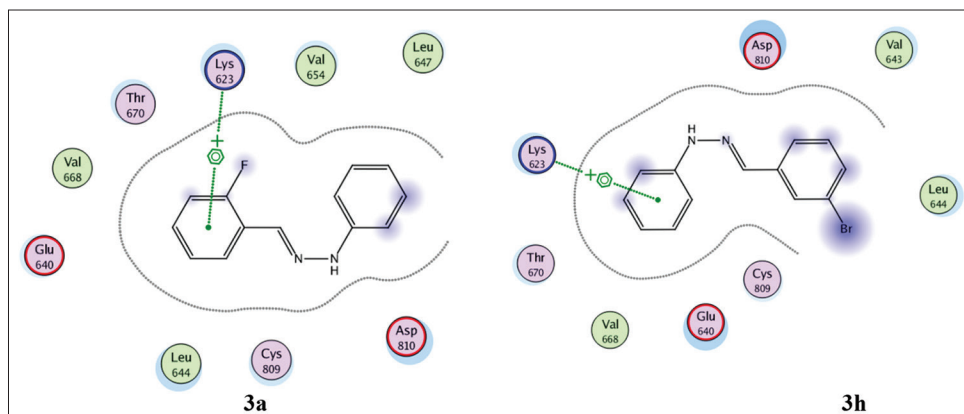


Figure 4: Spatial arrangement of compound 3a and 3h

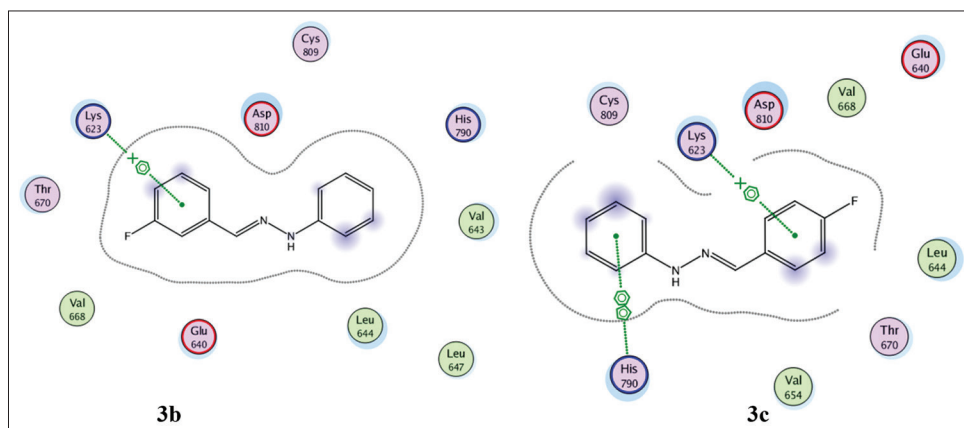


Figure 5: Spatial arrangement of compound 3b and 3c

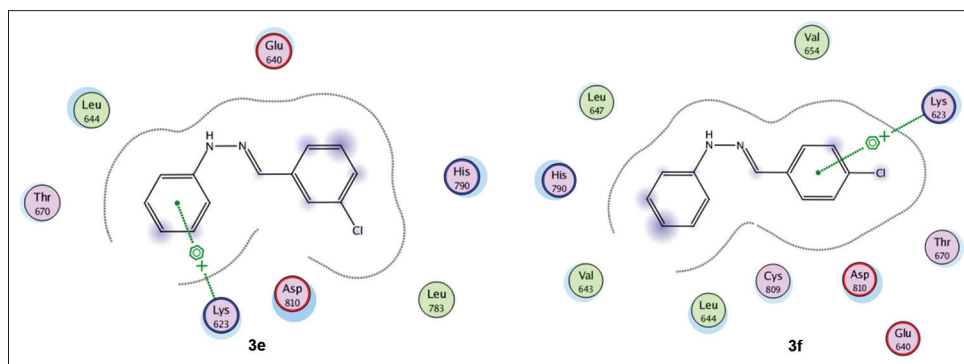


Figure 6: Spatial arrangement of compound 3e and 3f

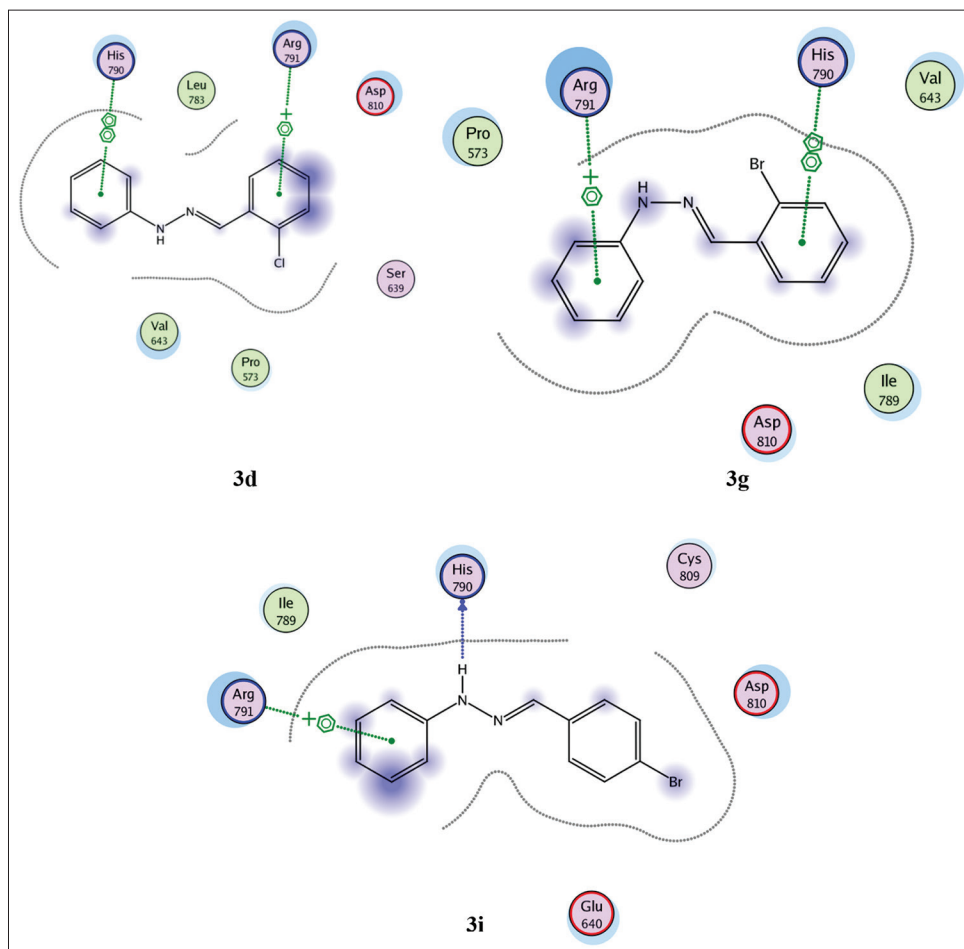


Figure 7A: Spatial arrangement of compound 3d, 3f and 3h

each compound. Superimposition of these compounds is presented in Figure 8.

Molecular Dynamic

Base on docking results, the stability of estimated active compounds, i.e., **3d**, **3g**, and **3i** were observed using MD simulation. The main purpose of MD simulation was to examine and also to confirm the binding profile of the

estimated active compound, in this research, MD simulation was run on 50 ns. MD simulation was also performed to ensure that interaction between protein and active compounds are still maintained.^[21] The high stability of those ligands was selected with the lowest energy minimum at temperature of 300K, it is observed the affinity of the ligand to binding site.

The efficiency of hydrogen bonding was examined before and after 50 ns and 300K MD simulations. In

general, the best conformation of compounds **3d**, **3g**, and **3i** will keep maintaining the interaction between ligand and receptor before and after MD simulation. Based on the stability of these three compounds and the Hydrogen bond

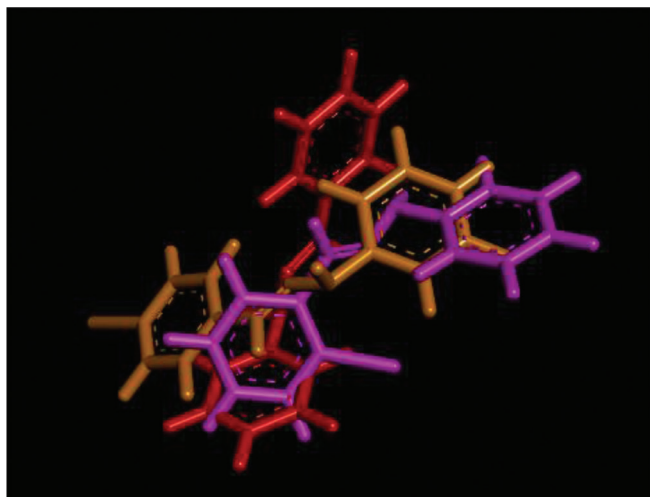


Figure 7B: Spatial arrangement of compound 3d, 3f and 3h

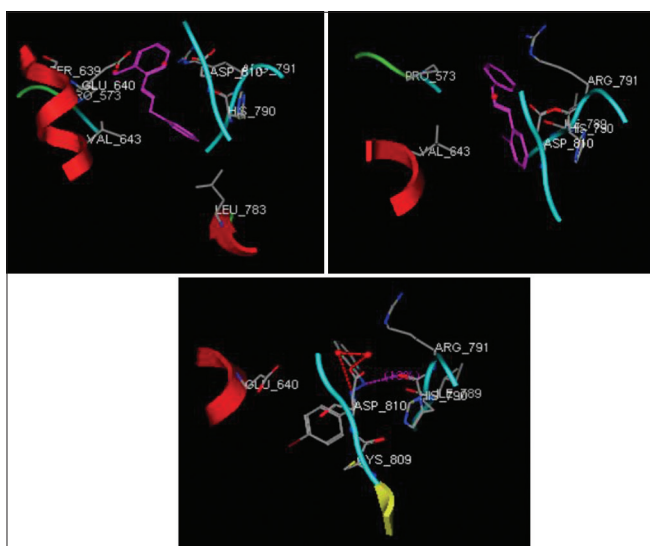


Figure 8: Visualization of MD interaction for compound 3d, 3g and 3i

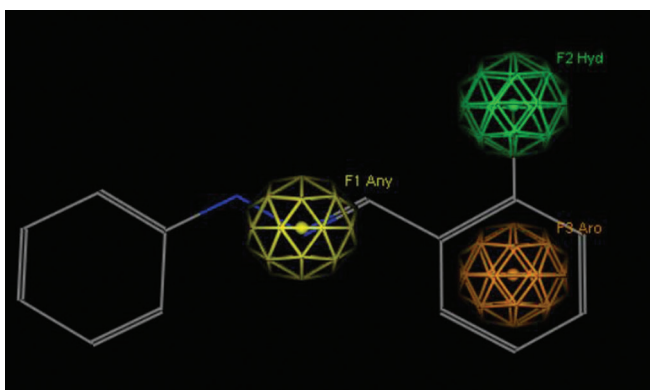


Figure 9: Best pharmacophore hypothesis yellow sphere is featured for hydrogen bond donor, green sphere for hydrophobic and orange sphere for aromatic ring

distance of these compounds are less than 2.9 Å, indicated that these complexes ligand-protein were stable and flexible. Based on MD simulation, **3d**, **3g**, and **3i** seemed to retain their interactions with the same amino acids after simulation. It is estimated that these compounds have big potency as breast cancer inhibitors. Interaction of MD simulation are depicted in Figure 9. Nevertheless, the rest of compounds lost their activity and the presence of the amino acids was also not maintained. Table 3 is listed the interactions with amino acids after the MD simulation.

Pharmacophore

Pharmacophore can be defined as the features of the steric and electronic ensemble that is very crucial and important to certify the interaction of the supramolecular with a biological target. In this study, we have identified the pharmacophore features as depicted in Figure 9. There are three features that were achieved, they are hydrophobic (green), hydrogen bond donor (yellow), and aromatic ring (orange). It is indicated that these features play an important role become active compounds.

Druglikeness Properties

The result of drug-likeness prediction using Swiss-ADME server showed that all halogenated hydrazones have very good drug-likeness properties with obey the Lipinski's, Ghose's, Veber's, Egan's, and Muegge rules. The drug-likeness properties were presented in Table 4.

In silico Toxicity Prediction

The HepG2 and hERG data in the Table 5 showed that the halogenated hydrazone series did not showed the hepatotoxicity and cardiotoxicity potencies, respectively. However, the MMP and AMES test data showed that two synthesized compounds (**3a** and **3g**) have potency of mitochondrial toxicity and also mutagenicity, while compound **3e** only showed the potency of mitochondrial toxicity and compounds **3b** and **3c** only showed the mutagenicity potency. Then, we also predicted the MRTD in mg/day for each compound using this server. The result showed that the difference in types and positions of halogen substituents

Table 3: Listed of the interactions with amino acids before and after MD simulation

Compound	Docking	MD	H bond distance
3a	Lys623	-	3.2 Å
3b	Lys623	-	3.5 Å
3c	Lys623	-	3.4 Å
3d	His790, Arg791	His790, Arg791	2.9 Å
3e	Lys623	-	3.2 Å
3f	Lys623	-	3.2 Å
3g	His790, Arg791	His790, Arg791	2.9 Å
3h	Lys623	-	3.5 Å
3i	His790, Arg791	His790, Arg791	2.9 Å
Doxorubicin	Tyr672, Asp677	Tyr672, Asp677	2.9 Å

Table 4: The drug-likeness properties of halogenated hydrazone series

Compounds	MW (g/mol)	H Bond Donor	H Bond Acceptor	Log P	Rotatable bond	TPSA (Å ²)	Druglikeness
3a	214.24	1	2	3.55	3	24.39	Yes
3b	214.24	1	2	3.55	3	24.39	Yes
3c	214.24	1	2	3.55	3	24.39	Yes
3d	230.69	1	1	3.68	3	24.39	Yes
3e	230.69	1	1	3.68	3	24.39	Yes
3f	230.69	1	1	3.68	3	24.39	Yes
3g	275.14	1	1	3.81	3	24.39	Yes
3h	275.14	1	1	3.81	3	24.39	Yes
3i	275.14	1	1	3.81	3	24.39	Yes

Table 5: The result of *in silico* toxicity prediction of halogenated hydrazone series

Compounds	Toxicity predictions				
	HepG2	hERG	MMP	AMES Test	MRTD
3a	No	No	Yes	Yes	58
3b	No	No	No	Yes	63
3c	No	No	No	Yes	101
3d	No	No	No	No	62
3e	No	No	Yes	No	68
3f	No	No	No	No	108
3g	No	No	Yes	Yes	74
3h	No	No	No	No	81
3i	No	No	No	No	129

affected the MRTD value of halogenated hydrazine series. We observed two trends. Firstly, the *para* halogenated hydrazones showed the higher MRTD value than *meta* and *ortho* halogenated hydrazones. This trend might be caused by the decreasing of negative inductive effect of halogen atoms with the increasing of bond distance between halogen substituent and azomethine group. Secondly, the fluoro substituted hydrazones showed the lowest MRTD value. This trend might be caused by the electronegativity of fluor atom. Based on the combination of molecular docking, molecular dynamic, drug-likeness properties, and *in silico* toxicity studies, the compounds **3d** with chloro substituent in *ortho* position and compound **3i** with bromo substituent in *para* position showed good potency as active inhibitors for MCF-7 with the lowest toxicity risk.

CONCLUSION

The present study describes the synthesis of substituted hydrazone series and investigated their anticancer potency against breast cancer. The synthesized compounds were correspond to the structure of the expected target molecule based on the results of UV, FTIR, NMR, and GC-MS spectroscopic data analysis. Based on the combination of molecular docking, molecular dynamic, drug-likeness properties, and *in silico* toxicity studies, the compounds **3d** with chloro substituent in *ortho* position and compound **3i** with bromo substituent in *para* position showed good potency as active inhibitors for MCF-7 with lowest toxicity

risk. This strategy is an early stage for discover new drugs for then it can be used as breast cancer inhibitors. However, the *in vitro* and *in vivo* evaluations in further work are required to ensure the potencies of these halogenated hydrazone series.

ACKNOWLEDGMENTS

This work has been supported and funded by the Ministry of Research and Technology and Higher Education (KEMENRISTEK DIKTI) of the Republic of Indonesia through Basic Research Grant with contract number of 735/UN.19.5.1.3/PT.01.03/2019.

REFERENCES

- Pandey J, Pal R, Dwivedi A, Hajela K. Synthesis of some new diaryl and triaryl hydrazine derivatives as possible estrogen receptor modulators. *Arzneimittelforschung* 2002;52:39-44.
- Cocco MT, Con C, Lilliu V, Onnis V. Synthesis and *in vitro* antitumoral activity of new hydrazinopyrimidine-5-carbonitrile derivatives. *Bioorg Med Chem* 2005;1:366-72.
- Cui Z, Li Y, Ling Y, Huang J, Cui J, Wang R, Yang X. New class of potent antitumor acylhydrazone derivatives containing furan. *Eur J Med Chem* 2010;45:5576-84.
- Altıntop MD, Özdemir A, Turan-Zitouni G, İlgin S, Atlı Ö, İscan G, et al. Synthesis and biological evaluation of some hydrazone derivatives as new anticandidal and anticancer agents. *Eur J Med Chem* 2012;58:299-307.
- Verma G, Marella A, Shaquiquzzaman M, Akhtar M, Ali MR, Alam MM. A review exploring biological activities of hydrazones. *J Pharm Bioallied Sci* 2014;6:69-80.
- Ikhtiarudin I, Frimayanti N, Teruna HY, Zamri A. Microwave-assisted synthesis, molecular docking study and *in vitro* evaluation of halogen substituted flavonols against P388 murine leukemia cells. *AST Proceed Ser* 2017;1:375-81.
- Jasril J, Ikhtiarudin I, Zamri A, Teruna HY, Frimayanti N. New fluorinated chalcone and pyrazolines analogues: Synthesis, docking and molecular dynamic studies as anticancer agents. *Thai J Pharm Sci* 2017;41:93-8.
- Jasril J, Frimayanti N, Ikhtiarudin I. *In silico* studies of fluorinated chalcone and pyrazoline analogues as inhibitors for cervical cancer. *AIP Conf Proceed* 2019;2242:040008.
- Hernandes MZ, Cavalcanti SM, Moreira DR, de Azevedo WF Jr., Leite AC. Halogen atoms in the modern medicinal chemistry: Hints for the drug design. *Curr Drug Targets* 2010;11:303-14.
- Kontoyianni M, McClellan LM, Sokol GS. Evaluation of docking performance: Comparative data on docking algorithms. *J Med Chem* 2004;47:558-65.
- Wang R, Lu Y, Wang S. Comparative evaluation of 11

- scoring functions for molecular docking. *J Med Chem* 2003;4:2287-303.
12. Mufakkar M, Tahir MN, Tariq MI, Ahmad S, Sarfraz M. (E)-1-(4-Methoxy-benzylidene)-2-phenyl-hydrazine. *Acta Crystallogr Sect E Struct Rep Online* 2010;66:o1887.
 13. Shad HA, Tahir MN, Tariq MI, Sarfraz M, Ahmad S. (E)-1-(2-Nitro-benzylidene)-2-phenyl-hydrazine. *Acta Crystallogr Sect E Struct Rep Online* 2010;66:o1955.
 14. Tahir MN, Tariq MI, Tariq RH, Sarfraz M. (E)-1-(4-Chloro-benzylidene)-2-phenyl-hydrazine. *Acta Crystallogr Sect E Struct Rep Online* 2011;67:o2377.
 15. Jasril J, Teruna HY, Aisyah A, Nurlaili N, Hendra R. Microwave assisted synthesis and evaluation of toxicity and antioxidant activity of pyrazoline derivatives. *Ind J Chem* 2019;19:583-91.
 16. Lu Y, Hendra R, Oakley AJ, Keller PA. Efficient synthesis and antioxidant activity of coelenterazine analogues. *Tetrahedron Lett* 2014;55:6212-5.
 17. Afriana N, Frimayanti N, Zamri A, Jasril J. Microwave-assisted synthesis, antioxidant and toxicological evaluation of a hydrazone, 1-(4-chlorobenzylidene)-2-phenylhydrazine. *AJP Conf Proceed* 2020;1655:012036.
 18. Jasril J, Ikhtiarudin I, Nurulita Y, Nurisma. Microwave-assisted synthesis and antioxidant activity of an imine, (E)-1-(3-bromobenzylidene)-2-phenylhydrazine. *AIP Conf Proceed* 2019;2242:040041.
 19. Daina A, Michielin O, Zoete V. SwissADME: A free web tool to evaluate pharmacokinetics, drug-likeness and medicinal chemistry friendliness of small molecules. *Sci Rep* 2017;7:42717.
 20. Schyman P, Liu R, Desai V, Wallqvist A. vNN web server for ADMET predictions. *Front Pharmacol* 2017;8:889.
 21. Frimayanti N, Ikhtiarudin I, Dona R, Agustini TT, Murdiya F, Zamri A. A computational approach to drug discovery: Search for chalcone analogues as the potential candidate for anti colorectal cancer (HT29). *Walailak J Sci Technol* 2020;17:64-74.